HortScience 60(6):871–877. 2025. https://doi.org/10.21273/HORTSCI18492-25

Variation in Root System Architecture and Lead Accumulation in Sweetpotato (*Ipomoea batatas* L.) Cultivars Bayou Belle and Beauregard

Mae Ann Bravo, Marissa Barbosa, Lisa Arce, Brenda Tubana, and Don LaBonte
School of Plant, Environmental, and Soil Sciences, Louisiana State University, Baton Rouge, LA 70803, USA

Jack Baricuatro
Department of Chemistry and Physics, LSU-Shreveport, Shreveport, LA 71115, USA

Arthur Villordon
LSU AgCenter Sweet Potato Research Station, Chase, LA 71324, USA

Keywords. lateral roots, lead stress, root system architecture, storage root formation, tolerance

Abstract. **The primary objective of this work was to generate species-specific information about root system architecture (RSA) adaptations to simulated natural levels of lead (Pb) during the establishment phase and onset of storage root formation in sweetpotato. In two separate experiments repeated two times, sweetpotato cultivars Bayou Belle (BB) and Beauregard (BX) were grown on sand substrate and provided with 0.5X Hoagland's nutrient solution with varying levels of Pb: 0, 10, 20, and 30 $\text{mg}\cdot\text{L}^{-1}$. All experiments were arranged in randomized complete block design (RCBD) with four replications. In the first experiment, entire root systems were sampled at 5, 10, and 15 days to represent key adventitious root (AR) developmental stages. The cultivars displayed variation in RSA attributes. Cultivar BB consistently exhibited higher lateral root (LR) number and greater root length than BX under all treatment levels. In contrast, BX main root length (MRL) treated with 10 $\text{mg}\cdot\text{L}^{-1}$ Pb increased 83%, 21%, and 15% relative to the untreated controls at 5, 10, and 15 days, respectively. A second experiment was conducted to collect storage root samples at 50 days. Storage root length, width, and length-to-width ratio did not vary with Pb levels in both cultivars. However, there was a cultivar-specific variation in storage root Pb accumulation across Pb treatments. The cultivar BB did not exhibit variation in storage root Pb accumulation across Pb treatment levels. In contrast, the cultivar BX demonstrated a 200- and 300-fold Pb accumulation at 20 and 30 $\text{mg}\cdot\text{L}^{-1}$ Pb treatment levels relative to the untreated BX control plants and significantly higher relative to BB storage roots grown at similar levels. Results are consistent with the hypothesis that increased root mass is associated with low accumulation of Pb. This study provides the first documented evidence of sweetpotato RSA responses to Pb at concentrations commonly found in agricultural soils. The findings corroborate evidence from model systems and well-characterized species of genotype-specific variability in RSA adaptation to Pb presence. Linking RSA responses to Pb tolerance will support crop improvement efforts to develop cultivars with reduced Pb accumulation.**

The widespread buildup of toxic elements (TEs) in agricultural systems poses a growing challenge for human health and safe food production. Owing to natural weathering of rocks and anthropogenic sources such as mining, smelting, and agrochemical use, TEs are inadvertently introduced to the soil (Liu et al. 2018; Palansooriya et al. 2020). Among various TEs, lead (Pb) is one of the most toxic and is ubiquitously present in a wide variety of environments (Pourrut et al. 2011). A US Department of Agriculture Soil Conservation Service sampling of 3045 sites representing the major crop producing areas of the United States found the soil Pb content ranged from 6.5 to 64.4 $\text{mg}\cdot\text{kg}^{-1}$ (Holmgren et al. 1993). Elevated soil Pb concentrations exert adverse effects to the cellular morphology, chlorophyll content, transpiration, root length, and overall growth of plants (Gupta et al. 2010; Huang and Huang 2008; Maestri et al. 2010; Rani et al. 2024). Lead is known to passively enter plant roots, with Ca^{2+} ionic channels hypothesized as the most important pathway (Kohli et al. 2020). Supporting and contradicting evidence for this hypothesis is reviewed by Pourrut et al. (2011). Although certain species are capable of transferring Pb to their shoots, $\sim$90% of total Pb is maintained in plant roots (Kumar et al. 2017), which can act as an effective barrier against Pb translocation (Gupta et al. 2013; Sharma and Dubey 2005). This root-based retention mechanism underscores the importance of understanding how root systems adapt to the presence of Pb in the soil. Such knowledge is vital for food safety, as it has been demonstrated that root crops accumulate more Pb in edible tissue compared with tuber and fruit crops grown in metal-rich soils (Byers et al. 2020).

A scrutiny of root system response to natural levels of Pb and other TEs is crucial for developing effective management practices and identifying desirable crop traits that enhance food safety and protect human health. RSA adapts to abiotic stress such as soil Pb contamination by altering root volume and diameter (Hou et al. 2022). These changes include inhibition of primary root and LR development, along with a reduction in the number of AR and LR density, which consequently decreases the total root volume (Hou et al. 2022; Ortiz-Luevano et al. 2021). Genotype-specific variation in RSA response to lead presence has been reported previously in rice (*Oryza sativa* L.) (Yang et al. 2000), sunflower (*Helianthus annuus* L.) (Strubińska and Hanaka 2011), and *Arabidopsis* (Ortiz-Luevano et al. 2021). RSA traits have been implicated in tolerance mechanisms in response to Pb presence. For example, Yang et al. (2000) reported that AR formation was associated with Pb-tolerant rice varieties. In sweetpotato (*Ipomoea batatas* L.), the successful emergence and development of LRs underpin the ability of AR to develop into storage roots (Villordon et al. 2012). Cumulative data support the hypothesis that optimized AR and LR number are RSA traits associated with the competency for early storage root formation in sweetpotato (Villordon et al. 2012). The global significance of sweetpotato highlights the need to investigate the environmental factors that influence RSA development and storage root formation. Two main objectives guide this study: 1) to characterize sweetpotato RSA response to simulated natural levels of Pb present in agricultural soils during the critical storage root initiation period, and 2) to measure Pb concentrations in different cultivars during the storage root bulking phase.

Materials and Methods

Plant materials and experimental conditions. The greenhouse experiments were performed at the LSU AgCenter Sweet Potato Research Station, in Chase, LA, USA (32°6′N, 91°42′W). Two pot experiments with two replicate studies per experiment were conducted (Table 1). The first experiment (PD1) was established for measuring RSA attributes at three timepoints: 5, 10, and 15 d (Table 1). These timepoints correspond to key developmental stages of storage root formation in 'Beauregard' sweetpotato: timing of plant establishment (emergence of ARs) (5 d), initial RSA development (10 d), and onset of storage root formation (15 d) (Villordon et al. 2009a,

Table 1. List of experiments.

Expt.	Study	Date planted	Date(s) harvested	Measurements/time points
1	A	20 Jan 2023	25 Jan 2023	Adventitious root count, lateral root length, lateral root density.
			30 Jan 2023	
			4 Feb 2023	5, 10, and 15 d
	B	23 Feb 2023	28 Feb 2023	
			5 Mar 2023	
			11 Mar 2023	
2	A	20 Jan 2023	10 Mar 2023	Storage root length, width, length/width ratio, lead accumulation.
	B	23 Feb 2023	14 Mar 2023	
				50 d

2009b). The second experiment (PD2) was to measure storage root attributes and Pb accumulation in storage roots at 50 d (Table 1). The following cultivars were used: BX (Rolston et al. 1987) and BB (LaBonte et al. 2013). The cultivar BX is a copper-skinned, orange-fleshed cultivar that is grown globally. BB is a red-skinned, orange-fleshed cultivar that was released specifically for processing. Virus-tested generation 1 storage roots were bedded in plastic containers containing substrate (Sungro; Sun Gro Horticulture, Bellevue, WA, USA) and served as a source of transplants or vegetative cuttings for subsequent experiments. In each experiment, cuttings were set in 10-cm-diameter PVC pots (height = 30 cm) with detachable plastic bottoms. Each plastic bottom had five drain holes, each measuring 2 mm in diameter. In addition, each PVC pot had four rows of side drain holes (2 mm in diameter; 3 cm apart within row) that were located diametrically opposite each other. These side drain holes were added to help reduce the incidence of a perched water table (Bilderback and Fonteno 1987). Washed river sand was used as a substrate for all experiments. Previous work has established that, for plants grown in this substrate, the time needed for plant establishment and storage root formation tracks key root developmental stages of field-grown plants (Villordon et al. 2009b). The diameter of the sand particles varied from 0.05 to 0.9 mm, with most (83%) in the 0.2- to 0.9-mm range. Substrate samples were submitted for toxic element laboratory analysis (Environmental Hazards Services, Richmond, VA, USA). In all experiments, vegetative terminal cuttings with the following characteristics were used: 25 to 30 cm in length, five to six fully opened leaves, ~5-mm diameter at the basal cut, and with uniform distribution of nodes.

All pots were provided with 0.5X Hoagland's No. 1 solution with nitrates as nitrogen source (Hoagland and Arnon 1950) with the following experimental treatments: 0, 10, 20, and 30 mg·L^{-1} Pb applied as lead (II) acetate trihydrate, Pb(CH$_3$COO)$_2$·3H$_2$O. These treatment levels were meant to simulate the range of Pb concentrations in sweetpotato-growing regions in the United States (Holmgren et al. 1993). A replicated sampling of commercial conventional and organic sweetpotato-producing locations in Louisiana and Mississippi in 2023 and 2024 showed that Pb levels ranged from 4.1 to 22 mg·L^{-1} (Bravo M, unpublished data), corroborating published data by Holmgren et al. (1993). During the critical establishment stage, specifically the first 3 days, 150 mL of the nutrient solution was provided daily. After establishment, 200 mL was provided every other day until the completion of the study. This protocol is equivalent to providing 25 mm·ha^{-1} of water with each application. Cuttings were planted to a uniform depth of 6 cm with two (BX) to three (BB) nodes beneath the substrate. All experiments were arranged in an RCBD repeated across planting dates. Unless otherwise indicated, each experiment had four replicates, with one plant per PVC pot constituting = one replicate.

Substrate moisture was measured with ECH2O soil moisture sensors inserted vertically at 2- to 7-cm depth (Model EC-5; Decagon Devices Inc., Pullman, WA, USA). The moisture of the substrate ranged from 5% to 9% volumetric water content (VWC) where ≈50% of field capacity is 7% VWC. At saturation, the substrate typically ranged from 12% to 14% VWC (Villordon et al. 2012). The greenhouse temperature regime for the first planting date was 28 °C (SD = 2) for 14 h at daytime and 24 °C (SD = 3) for 10 h at nighttime. The relative humidity (RH), measured hourly, averaged 59% (SD = 13.4). The temperature regime for the second planting date was 31 °C (SD = 2) for 14 h at daytime and 27 °C (SD = 2) for 10 h at nighttime. The RH averaged 53% (SD = 16). The temperature and RH were monitored at the canopy level using an integrated temperature and RH sensor (Model RHT, Decagon Devices Inc.). Supplementary lighting was provided using LED grow lights (Lumigrow Inc., Emeryville, CA, USA) for 14 h per day. Photosynthetic photon flux (PPF) for PD1 ranged from 200 to 1300 µmol·m^{-2}·s^{-1}; PPF for PD2 ranged from 277 to 1700 µmol·m^{-2}·s^{-1}. PPF was measured at the canopy level with a quantum sensor (Model QSO-S, Decagon Devices Inc.). These experimental approaches have been used to validate storage root initiation timing in BX (Villordon et al. 2009a, 2012) and measuring root architecture responses to biotic and abiotic variables (Villordon and Clark 2014, 2018; Villordon et al. 2012, 2013).

RSA measurements. During each sampling, the detachable plastic bottoms were removed, and the pot was tilted to gradually wash away the substrate with a stream of water. The roots were then placed in water-filled trays and rinsed twice. The AR samples were stored in 50% ethanol solution before scanning. Storage root formation at 15 d was confirmed by verifying the onset of anomalous cambium development in representative BX AR samples with diameter ≥2 mm (Villordon et al. 2020). Anomalous cambium development was verified by obtaining a cross-section 2.5 cm from the base of the AR, staining with toluidine blue, viewing under the microscope, and confirming the presence of circular anomalous cambia around the central metaxylem cell as well as around discrete protoxylem elements (Villordon et al. 2009a).

Measurement of root architectural attributes followed the procedures described in prior work (Villordon et al. 2020). Briefly, intact washed AR samples were floated on waterproof trays and scanned using an Epson Perfection V850 Pro Photo Scanner (Epson Corporation, Los Alamitos, CA, USA). Image acquisition parameter was set to "high" accuracy (600 dpi; image size ≈18 MB) and analysis precision was set to "high."

In prior work using the cultivar BX, preset intervals were used to classify root classes (Villordon et al. 2012, 2013); however, the variation in complexity of root samples among cultivars and overlapping root thickness necessitated modifications of prior approaches. For purposes of this work, AR specimens with labeled sections in Fig. 1 were used to standardize terminologies and clarify specific root class categories and measured attributes. First, main or primary root length (MRL) (Fig. 1A–C) was manually measured using the segmented line feature in ImageJ (Schneider et al. 2012). Second, total root length (TRL) was measured using Rhizovision Explorer (Seethepalli and York 2020). Debris such as sand particles and loose root tissue were excluded from the analysis by turning on the filter for nonroot objects in RhizoVision Explorer (size = 25 pixels). Finally, LR length (LRL) (Fig. 1A–C) was calculated by subtracting the manual MRL measurements from TRL.

Received for publication 5 Feb 2025. Accepted for publication 25 Mar 2025.

Approved for publication by the Director of the Louisiana Agricultural Experiment Station as manuscript number 2025-260-39864. Mention of trademark, proprietary product or method, and vendor does not imply endorsement by the Louisiana State University Agricultural Center nor its approval to the exclusion of other suitable products or vendors. This research was funded by Gerber Products Co. Portions of this research were also supported by the US Department of Agriculture's (USDA) Agricultural Marketing Service through grant AM22SCBPLA1142-00 and the Louisiana Sweetpotato Advertising and Development Fund. This material is based on work that is supported by the National Institute of Food and Agriculture, USDA, Hatch projects. We thank Cole Gregorie for the assistance in the conduct of the studies. We also thank Karsten Newby, who managed the work at Brooks Applied Labs.

M.A.B., M.B., and L.A. are graduate students.
B.T. and D.L. are professors.
J.B. is an assistant professor.
A.V. is the corresponding author. E-mail: avillordon@agcenter.lsu.edu.

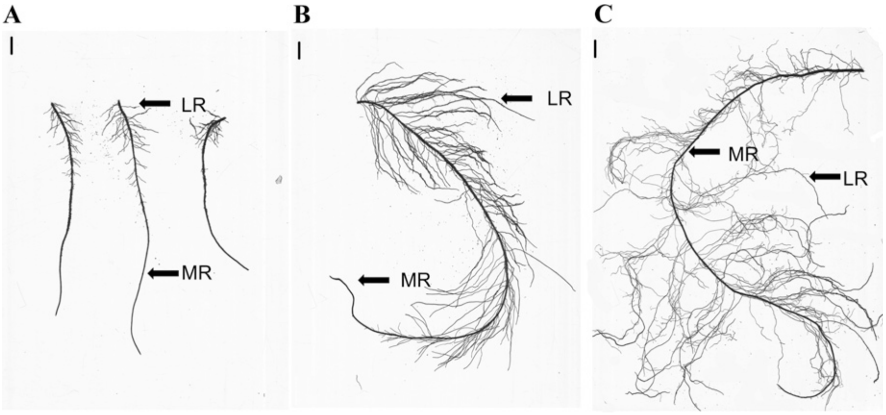

Fig. 1. Adventitious roots of sweetpotato cultivar Bayou Belle sampled at 5 (**A**), 10 (**B**), and 15 d (**C**) from plants grown without lead (Pb) treatment (control group). (**A**) shows adventitious root samples from a single plant. The main root (MR) and first-order lateral root (LR) are labeled in each plate to clarify terminology used throughout this report. Scale bar = 1 cm.

Storage root shape measurements and lead analysis. Storage roots sampled at 50 d were photographed and images were digitally analyzed using ImageJ (Schneider et al. 2012). The segmented line feature was used to measure storage root length, whereas the straight-line feature was used to measure storage root diameter. Length/width ratio was subsequently calculated. Unpeeled storage roots were washed with deionized water and sent to Brooks Applied Laboratories (Seattle, WA, USA) for Pb bulk analysis. All samples were homogenized using commercial laboratory equipment and then processed using a modified version of the Association of Official Analytical Collaboration (AOAC) 2015.01 Heavy Metals in Food method (Briscoe 2015). Briefly, aliquots of each sample homogenate were digested in a laboratory microwave system using concentrated nitric acid and hydrogen peroxide. The resulting sample digests were then analyzed for toxic element content using triple quadrupole inductively coupled plasma mass spectrometry, wherein multiple collision and/or reaction gases are used to eliminate polyatomic or isobaric interferences.

Statistical analyses. MRL, LRL, and storage root Pb accumulation were log 10 transformed, and AR and LR count data were square transformed before analysis. Statistical analyses were performed on transformed values using SAS mixed linear models procedure Proc Mixed (SAS 9.4; SAS Inc., Cary, NC, USA). Fisher's least significant difference test at the 0.05 *P* level was used to test for statistical significance. We failed to detect a significant planting date and cultivar effects on all root attributes; hence, data were combined. To visually assess RSA response and variability patterns within the RSA data, the R package ggplot2 (Wickham 2009) was used to generate boxplots using R Studio (v.1.2.1335; R Studio Inc., Boston, MA, USA) with R version 3.6 (R Development Core Team 2019). The data presented were from nontransformed data.

Results and Discussion

AR number. The cultivars generally manifested variable responses. BX demonstrated a decrease in the number of ARs at 5 and 10 d when treated with 10 mg·L^{-1} Pb (Fig. 2A and B). No significant differences in the number of ARs were detected in the cultivar BB between treatments across timepoints. The effects of Pb on AR emergence remain scant in other plant or crop species. Pb-tolerant rice varieties were found to develop AR, whereas Pb-sensitive ones failed to form AR even after 15 d (Yang et al. 2000). In sunflower (*Healianthus annuus* L.), AR formation was associated with Pb tolerance (Strubińska and Hanaka 2011). Yang et al. (2000) documented the compensatory formation of ARs in tolerant rice varieties after the inhibition of initial root growth, a feature lacking in nontolerant varieties. This compensatory root growth has been documented as a response to Pb stress in rhizomes in the clonally propagated *Phragmites australis* (Zhang et al. 2015).

The successful emergence of AR is crucial for sweetpotato commercial propagation and storage root yield. AR may develop from preformed nodes or basal cut ends within 3 to 5 days, depending on the cultivar (Ma et al. 2015; Villordon et al. 2009). Prior work of Ma et al. (2015) and Lowe and Wilson (1974) indicates no direct correlation between total AR number per plant and final storage root number at harvest in sweetpotato. Variations in AR number at establishment among sweetpotato cultivars has also been reported (Lowe and Wilson 1974; Nakatani and Watanabe 1986). The emergence of additional ARs over the next 10 d depends on genotype and environmental conditions, whereas the final storage roots yield is affected by assimilate production and transport (Lowe and Wilson 1974). Villordon et al. (2012) previously documented that cultivar-specific AR emergence is influenced by differences in ethylene sensitivity. Ethylene has been demonstrated to regulate Pb stress response in the root systems of *Arabidopsis* (Cao et al. 2009). Additional work is necessary to explore the role of cultivar-specific ethylene sensitivity in Pb tolerance in sweetpotato.

MRL. MRL in cultivar BB remained unchanged across all Pb treatment levels. In contrast, cultivar BX revealed 83%, 21%, and 15% increases in response to 10 mg·L^{-1} Pb at 5, 10, and 15 d, respectively, relative to the control plants (Fig. 3A–C). A cultivar-specific stimulatory effect on root growth

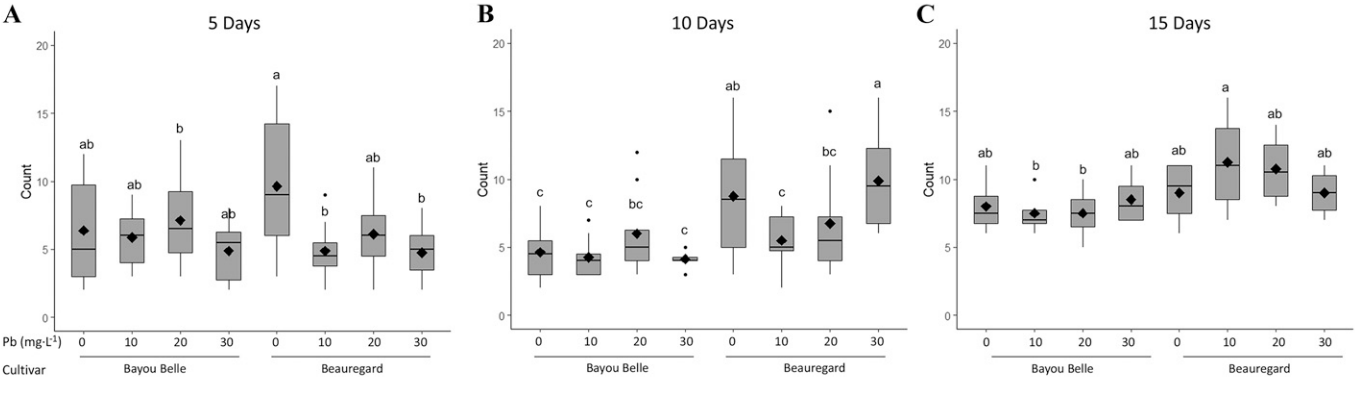

Fig. 2. Box plots of adventitious root number in sweetpotato cultivars treated with lead (Pb) at four different concentrations from two planting dates. Boxes represent the interquartile range (IQR, or middle 50%) of values for each feature. Shaded diamonds represent mean values. Bold horizontal lines indicate median values. Upper box plot whiskers represent the last data point within the range of 75% quantile +1.5 IQR, lower box plot whiskers represent the last data point within the range of 25% quantile–1.5 IQR. Dots represent outliers (values smaller or larger than the median ± 1.5 times the IQR). Boxes with different letters are significantly different based on Fisher's least significant difference mean separation test ($P < 0.05$).

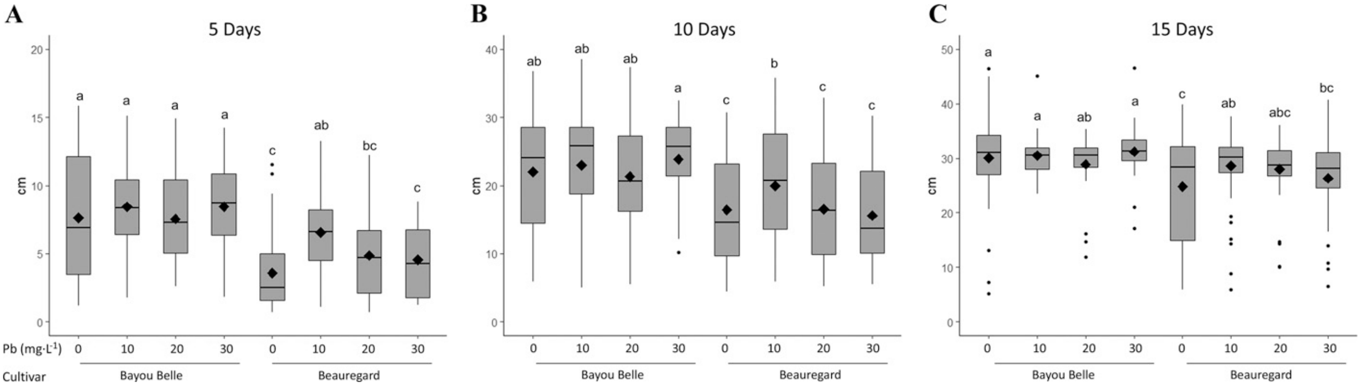

Fig. 3. Box plots of main root length of sweetpotato cultivars treated with lead (Pb) at four different concentrations from two planting dates. Boxes represent the interquartile range (IQR, or middle 50%) of values for each feature. Shaded diamonds represent mean values. Bold horizontal lines indicate median values. Upper box plot whiskers represent the last data point within the range of 75% quantile +1.5 IQR, lower box plot whiskers represent the last data point within the range of 25% quantile–1.5 IQR. Dots represent outliers (values smaller or larger than the median ± 1.5 times the IQR). Boxes with different letters are significantly different based on Fisher's least significant difference mean separation test ($P < 0.05$).

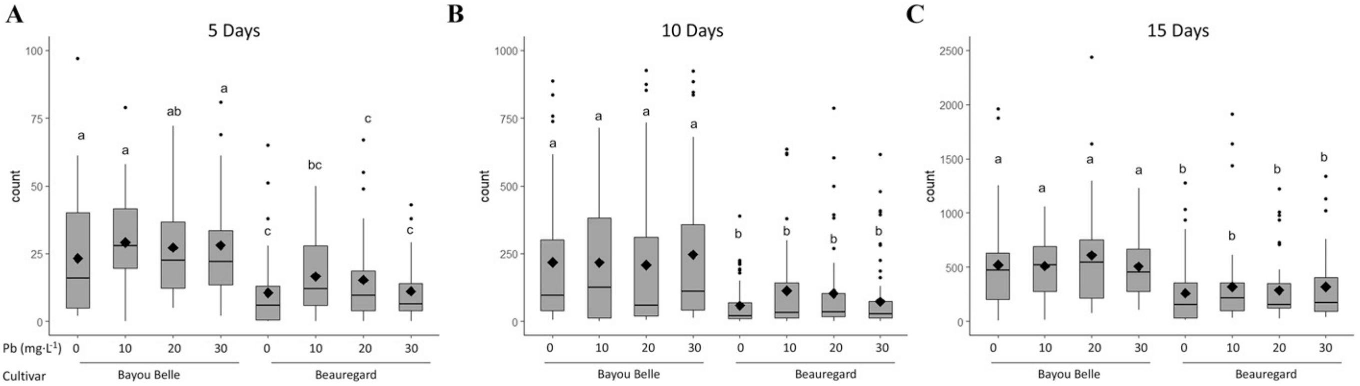

Fig. 4. Box plots of lateral root count of sweetpotato cultivars treated with lead (Pb) at four different concentrations from two planting dates. Boxes represent the interquartile range (IQR, or middle 50%) of values for each feature. Shaded diamonds represent mean values. Bold horizontal lines indicate median values. Upper box plot whiskers represent the last data point within the range of 75% quantile +1.5 IQR, lower box plot whiskers represent the last data point within the range of 25% quantile–1.5 IQR. Dots represent outliers (values smaller or larger than the median ± 1.5 times the IQR). Boxes with different letters are significantly different based on Fisher's least significant difference mean separation test ($P < 0.05$).

was reported for *Arabidopsis* exposed to low concentrations of Pb (Ortiz-Luevano et al. 2021); the observation was ascribed to a biphasic dose-response behavior. This biphasic response, known as hormesis, is a conserved phenomenon in plants exposed to toxic element stress conditions, where low stress concentrations stimulate root growth, while higher concentrations have inhibitory effects (Ortiz-Luevano et al. 2021). Other species show Pb-sensitive MRL responses. Morel at al. (2009) found that Pb reduced root length of wild-type *Arabidopsis* but this effect was reversed in plantlets that overexpress the *Arabidopsis thaliana* Heavy

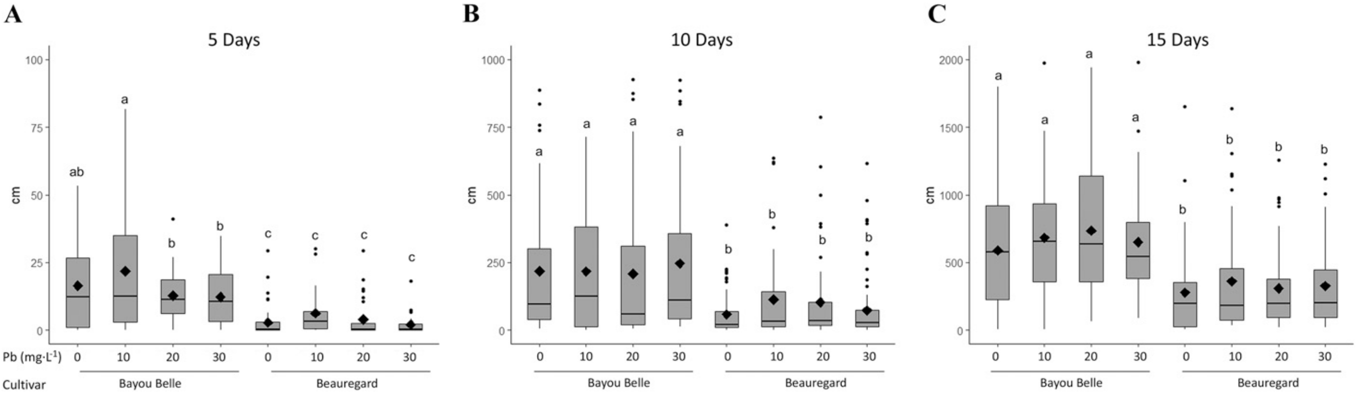

Fig. 5. Box plots of lateral root length of sweetpotato cultivars treated with lead (Pb) at four different concentrations from two planting dates. Shaded diamonds represent mean values. Bold horizontal lines indicate median values. Boxes represent the interquartile range (IQR, or middle 50%) of values for each feature. Upper box plot whiskers represent the last data point within the range of 75% quantile +1.5 IQR, lower box plot whiskers represent the last data point within the range of 25% quantile–1.5 IQR. Dots represent outliers (values smaller or larger than the median ± 1.5 times the IQR). Boxes with different letters are significantly different based on Fisher's least significant difference mean separation test ($P < 0.05$).

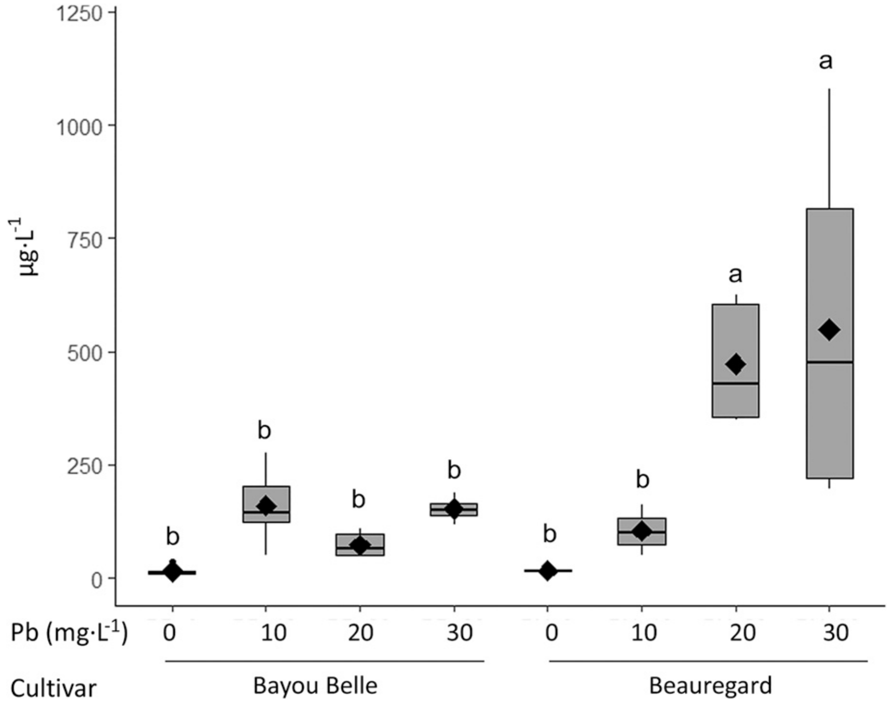

Fig. 6. Box plots of Pb accumulation of sweetpotato cultivars treated with lead (Pb) at four different concentrations from two planting dates. Shaded diamonds represent mean values. Bold horizontal lines indicate median values. Boxes represent the interquartile range (IQR, or middle 50%) of values for each feature. Upper box plot whiskers represent the last data point within the range of 75% quantile +1.5 IQR, lower box plot whiskers represent the last data point within the range of 25% quantile–1.5 IQR. Dots represent outliers (values smaller or larger than the median ± 1.5 times the IQR). Boxes with different letters are significantly different based on Fisher's least significant difference mean separation test ($P < 0.05$).

Metal Associated3 (AtHMA3) protein. AtHMA3 is involved in heavy metal transport and likely plays a role in the detoxification of heavy metals via vascular sequestration (Morel et al. 2009).

Root architecture attributes. No significant treatment effects were observed for the RSA traits within cultivars. However, cultivar BB consistently exhibited increased LR number and LRL compared with the control across Pb treatment levels and time points (Figs. 4 and 5). Such cultivar-dependent differences in LRL have been documented previously in the case of arsenic (Villordon et al. 2020; Villordon and Baricuatro 2024). Pb-induced RSA modifications were also noted in model systems. Exposure to Pb affected the development of *Arabidopsis* root system (Ortiz-Luevano et al. 2021) and caused a much denser and shorter LR system in maize (Obroucheva et al. 2001). Seregin et al. (2004) found trace amounts of Pb in the pericycle, suggesting metal tolerance of the root during branching.

Storage root responses and Pb accumulation. Cultivar BB did not show any variation in Pb accumulation across Pb treatment levels. However, cultivar BX accumulated Pb at levels 200 and 300 times higher at 20 and 30 mg·L^{-1} Pb, respectively, relative to the untreated controls (Fig. 6). There were no differences in storage root length, diameter, length/width ratio, and count at 50 d in both cultivars (Table 2). These observations are consistent with three prior findings. First, the biphasic response of cultivar BX toward Pb mimicked the trends in *Arabidopsis* (Ortiz-Luevano et al. 2021). Second, the reduced Pb accumulation in BB aligned with studies in other systems, where greater root biomass was associated with lower Pb uptake (Yang et al. 2000). This growth dilution effect was observed in pea (*Pisum sativum*), which showed increased yields at low Pb accumulation (Shabaan et al. 2020). Third, prior work demonstrated that Pb-induced variation in *Arabidopsis* RSA was genetically regulated and involved pathways shared with the inorganic phosphate (Pi) starvation response gene (PSR), implicating the role of Pi starvation-inducible gene *AtPHT1;4* (Ortiz-Luevano et al. 2021). Arce et al. (2024) recently demonstrated that sweetpotato cultivars grown in Pi-deficient conditions exhibit variations in the expression of PSR genes, notably the *Arabidopsis* ortholog *IbPHT1;4*. Ortiz-Luevano et al. (2021) also reported root exudate production by *Arabidopsis* grown in media supplemented with Pb. This novel molecular evidence, combined with reported variation in exudate production among sweetpotato cultivars grown in Pi-deficient conditions (Minemba et al. 2019), supports the cultivar-specific Pb response observed in this study. Furthermore, prior evidence also merits follow-up studies that test the hypothesis that BB and BX vary in exudate production in response to Pb presence. Reducing the bioavailability of TEs is a key step in the development of tolerance mechanisms in plants. Polyvalent anions with metal-chelating properties such as oxalates and malates can precipitate metal ions or form stable complexes that can prevent effective metal-ion translocation. In the case of Pb-tolerant rice, elevated levels of oxalates in the root and root exudates were observed and the addition of oxalate to the growth solution mitigated Pb-induced root growth inhibition (Yang et al. 2000).

The cultivars used in this study, as well as others bred under comparable conditions, possess an inherent adaptation to natural Pb levels. Variation in Pi sensing likely plays a role in cultivar-specific response to, and uptake of Pb. Further research is needed to validate these findings, especially in natural production environments. Such studies will deepen the molecular understanding of sweetpotato responses to Pb stress and steer the development of screening and selection methods toward the identification of low-Pb accumulating cultivars.

Conclusion

This report is the first to examine RSA responses of sweetpotato to Pb concentrations typical in agricultural soils. RSA modifications and Pb accumulation in storage roots are cultivar-dependent. The stimulation of root development at low Pb levels corroborates findings in the model systems and well-characterized crop species. The interactive effects of essential nutrients and plant response in modulating Pb uptake and accumulation highlight the need for standardized growth conditions in future investigations. Understanding root system adaptations, along with standardized experimental protocols, will support crop improvement efforts to develop cultivars with reduced Pb accumulation.

Table 2. Storage root attributes and count at 50 d in sweetpotato cultivars Bayou Belle and Beauregard grown with natural levels of lead (Pb).

Cultivar	Pb (mg·L^{-1})	Length (cm)	Diam (cm)	L/W	Count
Bayou Belle	0	7.5 ± 0.4 ab	1.4 ± 0.1 a	5.3 ± 0.2 abc	6.8 ± 1.1 a
	10	6.9 ± 0.7 abc	1.5 ± 0.1 a	4.8 ± 0.4 bcd	4.8 ± 1.1 a
	20	7.5 ± 0.9 ab	1.5 ± 0.1 a	5.5 ± 0.5 ab	4.0 ± 1.1 a
	30	8.1 ± 0.9 a	1.4 ± 0.1 a	6.1 ± 0.4 a	3.8 ± 0.8 a
Beauregard	0	5.5 ± 0.5 c	1.4 ± 0.1 a	4.2 ± 0.2 cde	5.3 ± 0.9 a
	10	6.0 ± 0.6 bc	1.4 ± 0.1 a	4.2 ± 0.4 cde	5.0 ± 1.1 a
	20	5.2 ± 0.4 c	1.5 ± 0.2 a	3.4 ± 0.5 e	4.8 ± 0.3 a
	30	5.7 ± 0.5 bc	1.5 ± 0.1 a	4.0 ± 0.3 de	4.5 ± 0.5 a

Values represent means (±*SE*). Means within columns followed by a common letter are not significantly different based on Fisher's least significant different means separation test ($P \leq 0.05$). Values were log^{10} transformed. Corresponding nontransformed values are shown. Storage root samples were collected 50 d after planting. L/W = Length/Width ratio.

References Cited

Arce LI, LaBonte D, Gregorie C, Villordon A. 2024. Differential expression of phosphate starvation-responsive genes among sweetpotato cultivars during establishment and onset of storage root formation. J Am Soc Hortic Sci. 149(6):311–319. https://doi.org/10.21273/JASHS05433-24.

Bilderback TE, Fonteno WC. 1987. Effects of container geometry and media physical properties on air and water volumes in containers. J Environ Hortic. 5(4):180–182. https://doi.org/10.24266/0738-2898-5.4.180.

Briscoe M. 2015. Determination of heavy metals in food by inductively coupled plasma–mass spectrometry: First action 2015.01. J AOAC Int. 98(4):1113–1120. https://doi.org/10.5740/jaoac.int.2015.01.

Byers HL, McHenry LJ, Grundl TJ. 2020. Increased risk for lead exposure in children through consumption of produce grown in urban soils. Sci Total Environ. 743:140414. https://doi.org/10.1016/j.scitotenv.2020.140414.

Cao S, Chen Z, Liu G, Jiang L, Yuan H, Ren G, Bian X, Jian H, Ma X. 2009. The Arabidopsis ethylene-insensitive 2 gene is required for lead resistance. Plant Physiol Biochem. 47(4):308–312. https://doi.org/10.1016/j.plaphy.2008.12.013.

Gupta DK, Huang G, Corpas FJ. 2013. Lead tolerance in plants: Strategies for phytoremediation. Environ Sci Pollut Res Int. 20(4):2150–2161. https://doi.org/10.1007/s11356-013-1485-4.

Gupta DK, Huang HG, Yang XE, Razafindrabe BHN, Inouhe M. 2010. The detoxification of lead in *Sedum alfredii* H. is not related to phytochelatins but the glutathione. J Hazard Mater. 177(1-3):437–444. https://doi.org/10.1016/j.jhazmat.2009.12.052.

Hoagland DR, Arnon DI. 1950. The water-culture method for growing plants without soil. Circular. California Agricultural Experiment Station, 347 (2nd ed.).

Huang TL, Huang HJ. 2008. ROS and CDPK-like kinase-mediated activation of MAP kinase in rice roots exposed to lead. Chemosphere. 71(7):1377–1385. https://doi.org/10.1016/j.chemosphere.2007.11.031.

Hou F, Liu K, Zhang N, Zou C, Yuan G, Gao S, Zhang M, Pan G, Ma L, Shen Y. 2022. Association mapping uncovers maize ZmbZIP107 regulating root system architecture and lead absorption under lead stress. Front Plant Sci. 13:1015151. https://doi.org/10.3389/fpls.2022.1015151.

Kohli SK, Handa N, Bali S, Khanna K, Arora S, Sharma A, Bhardwaj R. 2020. Current scenario of Pb toxicity in plants: Unraveling plethora of physiological responses, p 153–197. In: de Voogt P (ed). Reviews of environmental contamination and toxicology, Vol 249. Springer International Publishing, Cham, Switzerland. https://doi.org/10.1007/398_2019_25.

Kumar B, Smita K, Cumbal Flores L. 2017. Plant mediated detoxification of mercury and lead. Arab J Chem. 10:S2335–S2342. https://doi.org/10.1016/j.arabjc.2013.08.010.

Maestri E, Marmiroli M, Visioli G, Marmiroli N. 2010. Metal tolerance and hyperaccumulation: Costs and trade-offs between traits and environment. Environ Exp Bot. 68(1):1–13. https://doi.org/10.1016/j.envexpbot.2009.10.011.

Holmgren GGS, Meyer MW, Chaney RL, Daniels RB. 1993. Cadmium, lead, zinc, copper and nickel in agricultural soils of the United States of America. J Env Quality. 22(2):335–348. https://doi.org/10.2134/jeq1993.00472425002200020015x.

LaBonte DR, Villordon AQ, Smith T, Clark CA (inventors). 2013. Sweetpotato plant named '07-146'. Board of Supervisors of Louisiana State University and Agricultural and Mechanical College through the LSU AgCenter (assignee). US Plant Patent 23785P3. (Filed 22 Nov 2011, granted 30 Jul 2013).

Liu C, Wang L, Yin J, Qi L, Feng Y. 2018. Combined amendments of nano-hydroxyapatite immobilized cadmium in contaminated soil-potato (*Solanum tuberosum* L.) system. Bull Environ Contam Toxicol. 100(4):581–587. https://doi.org/10.1007/s00128-018-2299-3.

Lowe SB, Wilson LA. 1974. Comparative analysis of tuber development in six sweet potato (*Ipomoea batatas* (L.) Lam) cultivars: 1. Tuber initiation, tuber growth and partition of assimilate. Ann Bot. 38(2):307–317. https://doi.org/10.1093/oxfordjournals.aob.a084814.

Ma J, Aloni R, Villordon AQ, Labonte D, Kfir Y, Zemach H, Schwartz A, Althan L, Firon N. 2015. Adventitious root primordia formation and development in stem nodes of 'Georgia Jet' sweetpotato, *Ipomoea batatas*. Am J Bot. 102(7):1040–1049. https://doi.org/10.3732/ajb.1400505.

Minemba D, Gleeson DB, Veneklaas E, Ryan MH. 2019. Variation in morphological and physiological root traits and organic acid exudation of three sweet potato (*Ipomoea batatas*) cultivars under seven phosphorus levels. Sci Hortic. 256:108572. https://doi.org/10.1016/j.scienta.2019.108572.

Morel M, Crouzet J, Gravot A, Auroy P, Leonhardt N, Vavasseur A, Richaud P. 2009. AtHMA3, a P1B-ATPase allowing Cd/Zn/Co/Pb vacuolar storage in Arabidopsis. Plant Physiol. 149(2):894–904. https://doi.org/10.1104/pp.108.130294.

Nakatani M, Watanabe Y. 1986. Effects of soil temperatures on the rooting of cut-sprouts of sweet potato (*Ipomoea batatas* Lam.): I. Optimum soil temperature for rooting and effects of high soil temperatures on the physiological and anatomical characteristics of roots. Jpn J Crop Sci. 55(2):208–216. https://doi.org/10.1626/jcs.55.208.

Obroucheva NV, Ivanov VB, Sobotik M, Bergmann H, Antipova OV, Bystrova EI, Seregin IV, Shpigun LK. 2001. Lead effects on cereal roots in terms of cell growth, root architecture and metal accumulation, p 165–170. In: Gašparíková O, Čiamporová M, Mistrík I, Baluška F (eds). Recent advances of plant root structure and function. Springer, Dordrecht, Netherlands. https://doi.org/10.1007/978-94-017-2858-4_20.

Ortiz-Luevano R, López-Bucio J, Martínez-Trujillo M, Sánchez-Calderón L. 2021. Changes induced by lead in root system architecture of Arabidopsis seedlings are mediated by PDR2-LPR1/2 phosphate dependent way. Biometals. 34(3):603–620. https://doi.org/10.1007/s10534-021-00299-9.

Palansooriya KN, Shaheen SM, Chen SS, Tsang DCW, Hashimoto Y, Hou D, Bolan NS, Rinklebe J, Ok YS. 2020. Soil amendments for immobilization of potentially toxic elements in contaminated soils: A critical review. Environ Int. 134:105046. https://doi.org/10.1016/j.envint.2019.105046.

Pourrut B, Shahid M, Dumat C, Winterton P, Pinelli E. 2011. Lead uptake, toxicity, and detoxification in plants. Rev Environ Contam Toxicol. 213:113–136. https://doi.org/10.1007/978-1-4419-9860-6_4.

Rani M, Vikas Kumar R, Lathwal M, Kamboj A. 2024. Effect and responses of lead toxicity in plants, p 211–241. In: Kumar N, Jha AK (eds). Lead toxicity mitigation: sustainable nexus approaches. Springer Nature, Cham, Switzerland. https://doi.org/10.1007/978-3-031-46146-0_10.

Rolston LH, Clark CA, Cannon JM, Randle WM, Riley EG, Wilson PW, Robbins ML. 1987. 'Beauregard' Sweet Potato. HortScience. 22(6):1338–1339. https://doi.org/10.21273/HORTSCI.22.6.1338.

Schneider CA, Rasband WS, Eliceiri KW. 2012. NIH Image to ImageJ: 25 years of image analysis. Nat Methods. 9(7):671–675. https://doi.org/10.1038/nmeth.2089.

Seethepalli A, York LM. 2020. RhizoVision Explorer - interactive software for generalized root image analysis designed for everyone (Version 2.0.2). Zenodo. https://doi.org/10.5281/zenodo.4095629. [accessed 23 Feb 2025].

Seregin IV, Shpigun LK, Ivanov VB. 2004. Distribution and toxic effects of cadmium and lead on maize roots. Russ J Plant Physiol. 51(4):525–533. https://doi.org/10.1023/B:RUPP.0000035747.42399.84.

Shabaan M, Asghar HN, Akhtar MJ, Ali Q, Ejaz M. 2020. Role of plant growth promoting rhizobacteria in the alleviation of lead toxicity to *Pisum sativum* L. Int J Phytoremediation. 23(8):837–845. https://doi.org/10.1080/15226514.2020.1859988.

Sharma P, Dubey RS. 2005. Lead toxicity in plants. Braz J Plant Physiol. 17(1):35–52. https://doi.org/10.1590/S1677-04202005000100004.

Strubińska J, Hanaka A. 2011. Adventitious root system reduces lead uptake and oxidative stress in sunflower seedlings. Biologia plant. 55(4):771–774. https://doi.org/10.1007/s10535-011-0185-5.

Villordon AQ, Baricuatro J. 2024. Variation in root system architecture response to arsenic during establishment and onset of storage root formation in two sweetpotato (*Ipomoea batatas* L.) cultivars. HortScience. 59(4):489–495. https://doi.org/10.21273/HORTSCI17616-23.

Villordon A, Gregorie JC, LaBonte D. 2020. Variation in phosphorus availability, root architecture attributes, and onset of storage root formation among sweetpotato cultivars. HortScience. 55(12):1903–1911. https://doi.org/10.21273/HORTSCI15358-20.

Villordon A, Clark C. 2018. Variation in root architecture attributes at the onset of storage root formation among resistant and susceptible sweetpotato cultivars infected with *Meloidogyne incognita*. HortScience. 53(12):1924–1929. https://doi.org/10.21273/HORTSCI15358-20.

Villordon A, Clark C. 2014. Variation in virus symptom development and root architecture attributes at the onset of storage root initiation in 'Beauregard' sweetpotato plants grown with or without nitrogen. PLoS One. 9(9):e107384. https://doi.org/10.1371/journal.pone.0107384.

Villordon A, LaBonte D, Firon N, Carey E. 2013. Variation in nitrogen rate and local availability alter root architecture attributes at the onset of storage root initiation in 'Beauregard' sweetpotato. HortScience. 48(6):808–815. https://doi.org/10.21273/HORTSCI.48.6.808.

Villordon A, LaBonte D, Solis J, Firon N. 2012. Characterization of lateral root development at the onset of storage root initiation in 'Beauregard' sweetpotato adventitious roots. HortScience. 47(7):961–968. https://doi.org/10.21273/HORTSCI.47.7.961.

Villordon AQ, La Bonte DR, Firon N, Kfir Y, Pressman E, Schwartz A. 2009a. Characterization of adventitious root development in sweetpotato. HortScience. 44(3):651–655. https://doi.org/10.21273/HORTSCI.44.3.651.

Villordon A, LaBonte D, Firon N. 2009b. Development of a simple thermal time method for describing the onset of morpho-anatomical features related to sweetpotato storage root formation. Sci Hortic. 121(3):374–377. https://doi.org/10.1016/j.scienta.2009.02.013.

Yang YY, Jung JY, Song WY, Suh HS, Lee Y. 2000. Identification of rice varieties with high tolerance or sensitivity to lead and characterization of the mechanism of tolerance. Plant Physiol. 124(3):1019–1026. https://doi.org/10.1104/pp.124.3.1019.

Zhang N, Zhang JW, Yang YH, Li XY, Lin JX, Li ZL, Cheng Y, Wang JF, Mu CS, Wang AX. 2015. Effects of lead contamination on the clonal propagative ability of *Phragmites australis* (common reed) grown in wet and dry environments. Plant Biol. 17(4):893–903. https://doi.org/10.1111/plb.12317.